Some Dynamic Aspects of Weld Molten Metal in Electron Beam Welding†

Yoshiaki ARATA*, Fukuhisa MATSUDA and Takashi MURAKAMI*****

Abstract

Some fundamental researchs were carried out on the dynamic aspects of weld molten metal in electron beam welding. That is, the authors observed the shape of the piercing hole during welding by means of a pin-hole X-ray camera, exposed solidification interface by means of the instantaneous extrusion method, observed the flow of weld molten metal by means of insertion of dissimilar metals, studied dynamic behaviors in the surface of weld molten metal using a high speed picture and also studied the relations between the surface swellings of molten metal and the repetitions of spiking and weld bead ripple. From the results obtained in these experiments, authors showed the dynamic behaviors of molten metal during electron beam welding to a schematic diagram and discussed its welding mechanism.

1. Introduction

In histrical view, some reports on the behaviors of weld molten metal in electron beam welding were as follows: In 1965, Hashimoto and Matsuda presumed the piercing action of molten metal in electron beam welding by many kinds of experimental results[1]. In 1969, H. Tong confirmed the piercing action by means of instantaneous X-ray[2]. In 1972, McMaster and Funk photographed the penetration mechanism using X-ray high speed camera, observed the piercing action and moreover they confirmed that the hole is not static but dynamic[3]. Also in 1972, Taniguch and his members measured intensity of X-ray generated from surface and bottom of the hole.[4] Moreover in the same year, Nakane and his members studied the behaviors of weld molten metal[5]. As mentioned above, it has been confirmed that the hole is made in the molten pool during electron beam welding, the electron beam flow in it and from there X-ray is generated. However still now, it is not so clarified as the behaviors of weld molten metal and there are some unknown things, for example, spikings generated in welding and the relations between the stirring of molten metal and weld defects (porosity, cracking and etc.). In this paper the authors studied some dynamic behaviors of weld molten metal in electron beam welding by means of X-ray photograph, instantaneous extrusion method, inserted dissimilar metal and high speed camera.

Moreover in these experiments, the authors applied high voltage type electron beam welding machine (maximum power: 6 KW at 150 KV, 40 mA).

2. Observation of Shape of Piercing Hole Using X-ray Generated from Weld Molten Pool

In this chapter the authors photographed the X-ray generated from weld molten metal and discussed the relation between shape of piercing hole and X-ray intensity. **Fig. 1** is the sketch of a pin hole camera used. Test specimen is placed in left side, in right side the X-ray film cassette is setting and in the middle of both sides lead sheet (3 mm t) is placed to screen X-ray and in this center pin hole (1 mmϕ) is made. Moreover camera itself is surrounded all over by lead sheet. Test pieces are carbon steel, SB 49 (40 mm t), austenitic stainless steel, SUS 304 (40 mm t) and aluminium, 2S (40 mmt). X- ray film is SAKURA RR and standard developed.

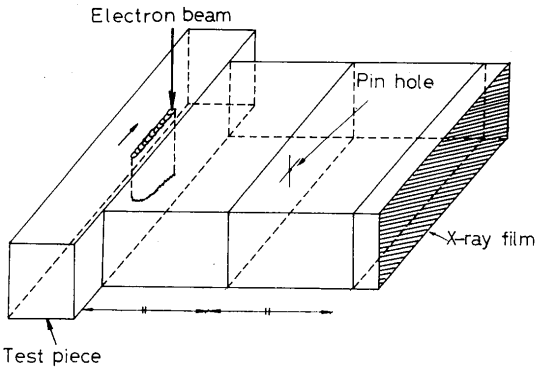

Fig. 1. Schmatic representation of pin hole camera used.

† Received on Aug. 3, 1973
* Professor
** Associate Professor
*** Graduate Student

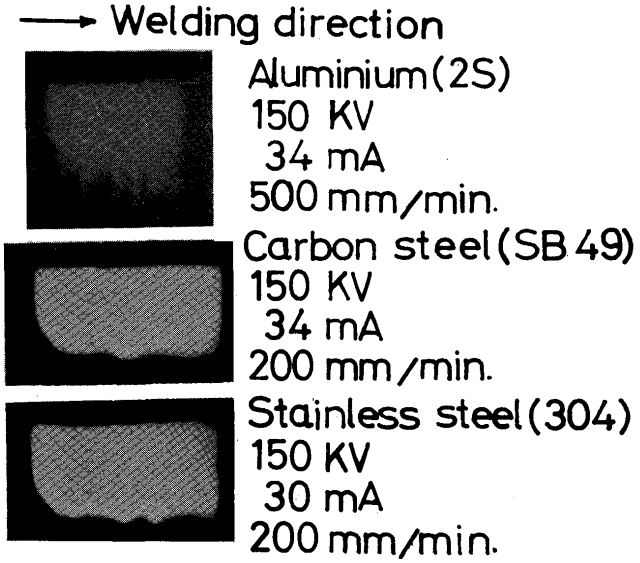

Photo. 1. Some examples of weld penetration shape on X-ray film which were photogrphed by the pin hole camera.

Welding bead length is about 30 mm. **Photo. 1** is examples photographed in this experiment. As shown in Photo. 1, white part indicates the penetration zone and upper part is top surface of the plate and under part is the tip of penetration depth. We cut the longitudinal section of each weld bead and observed the penetration shape. As a result, practical penetration depth is about from 1.3 to 1.4 times as deep as the picture photographed on X-ray film. Therefore it is clear that considerably much X-ray generates from about 70 % of practical penetration depth. Besides, it will become clear that X-ray generates from much more deep point of penetration shape improving the experimental method. In the case of Aluminium, it is photographed in comparatively deep color (white) at the point of spikings because of its much X-ray. This fact indicates that electron beam flow into weld molten pool strongly when spikings occur. That is, electron beam does not flow continuously and beam intensity varies fairly discontinuously in electron beam welding. This state is shown sketchily in **Fig. 2.**

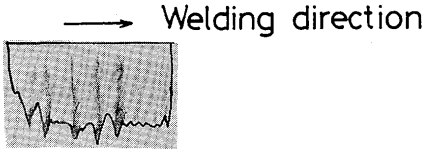

Fig. 2. Schematic representation of weld penetration shape photographed by the pin hole camera.

In this chapter these results are summarized as follows;

1) The picture photographed in X-ray film corresponded almost to practical penetration shape. Accordingly this method can be formed as a means by which we can understand the weld penetration shape non-destructively.
2) It can be directly indicated that molten pool is pierced to neighborhood of the tip of penetration depth in electron beam welding.
3) Also it can be seen light and shade on X-ray film periodically. Particularly it is photographed more deep in the part where spikings generate than another parts. That is, it is considered that quantity of electron beam which penetrates inside of metal varies for some reason and increase when spikings occur. Namely, it is understood that electron beam which flows in the molten pool varies always dynamically.

3. Observations of Solidification line by Instantaneous Extrusion Method

In this chapter, the authors observed the solidification line of some metals using instantaneous extrusion method to confirm the solidification line of molten pool in welding.

The experiment in chapter 2 was carried out to observe the surface condition of molten metal and so in this chapter it is to understand the variation of surface condition and solidification line. **Fig. 3** is the schematic diagram of the jig of instantaneous extrusion method.

The principle is as follows; small channel (length: 5 mm, dia.: 1 mm) is set perpendicularly from the bottom of test specimen and air tank is set at the back side of test specimen, when weld penetration reaches to the channel of test specimen in electron beam welding the air is extruded instantaneously to the outside, and as the result the metal of molten

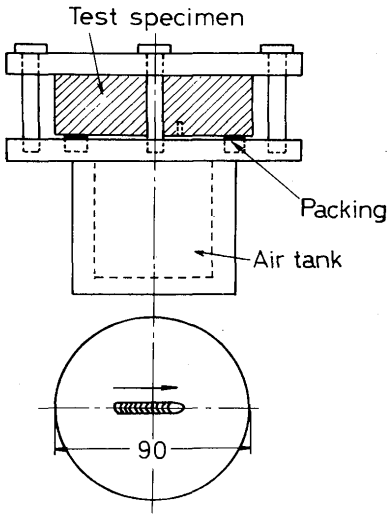

Fig. 3. Schematic diagram of instantaneous extrusion device used.

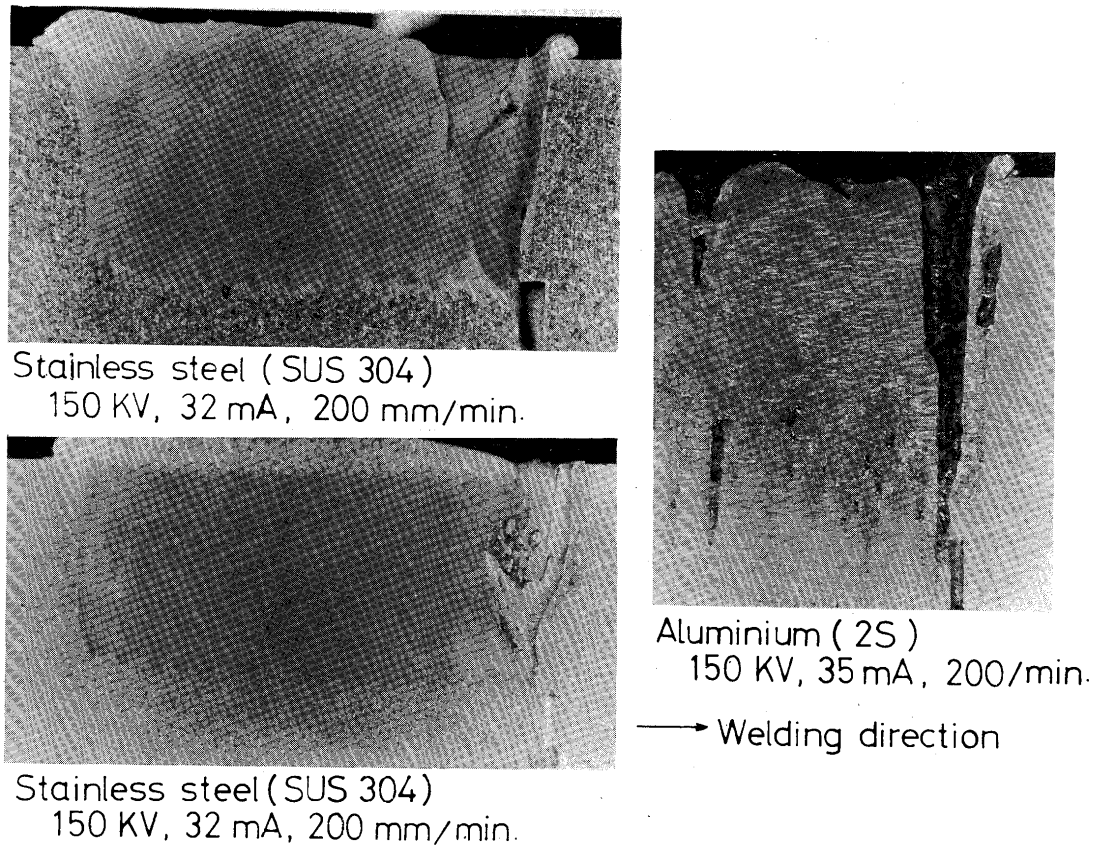

Photo. 2. Some examples of solidification interface which was obtained with the instantaneous extrusion method.

pool is extruded completely and solidification line exposes. Thus the authors observed the solidification interface. Test specimens used are carbon steel, austenitic stainless steel and pure aluminium (plate thickness; 20 and 30 mm). Some examples of solidification interface obtained in this experiment are shown in **Photo. 2.**

From these results it become clear that ripple lines which were usually seen in the longitudinal section of weld bead showed approximately the shape of solidification interface.

In this chapter these results summarized as follows;

1) The authors could expose the solidification line using our developed experimental method. As the result it became clear that ripple lines which were seen in the longitudinal section of weld bead showed the shape of solidification interface. The schematic diagram is shown in **Fig. 4.**

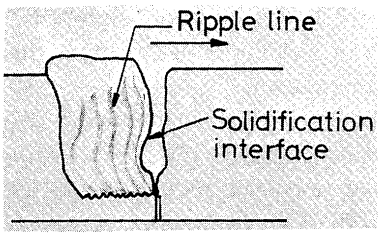

Fig. 4. Schematic representation of solidification interface and ripple line.

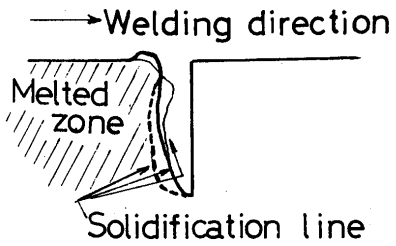

Fig. 5. Schematic representation of variation in transfiguration of solidification interface.

2) Concerning weld beads of the same welding condition, it became clear that solidification line mentioned above did not show always the same form but varied differently. The schematic representation is shown in **Fig. 5.**

4. Observations of Flow of Molten Metal in Weld Molten Pool

In this chapter the authors inserted stainless steel wire vertically (dia; 1.6 mm) to the bottom of carbon steel test specimen, melted in electron beam welding and observed the process of stainless steel molten metal flowing to carbon steel molten metal. **Fig. 6** shows the schematic diagram of experimental setting.

After welding, we cut the longitudinal section of

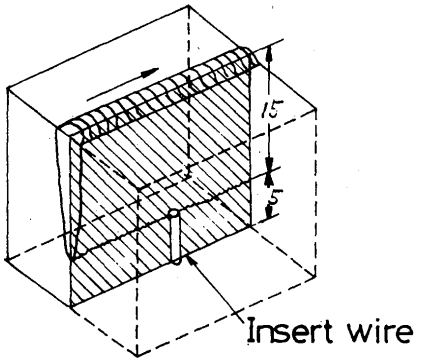

Fig. 6. Appearance of experimental setting for insert dissimilar metal.

weld bead and observed the process of stainless steel molten metal flowing to carbon steel molten metal. Longitudinal cutting positions and their macro-photographs are shown in **Fig. 7.** From the result of Fig. 7, the distribution of stainless steel molten metal in weld metal can be plotted as shown in **Fig. 8.**

In Fig. 7 (a), it is very peculiar that when stainless steel wire in bottom position is melted and flows upward, it branches to two flows at the bending position of upper melted zone. Namely it is seen that the one part passes the bending position, still more flows to flat part of upper side and the other part turns at the bending position and falls ahead to the welding

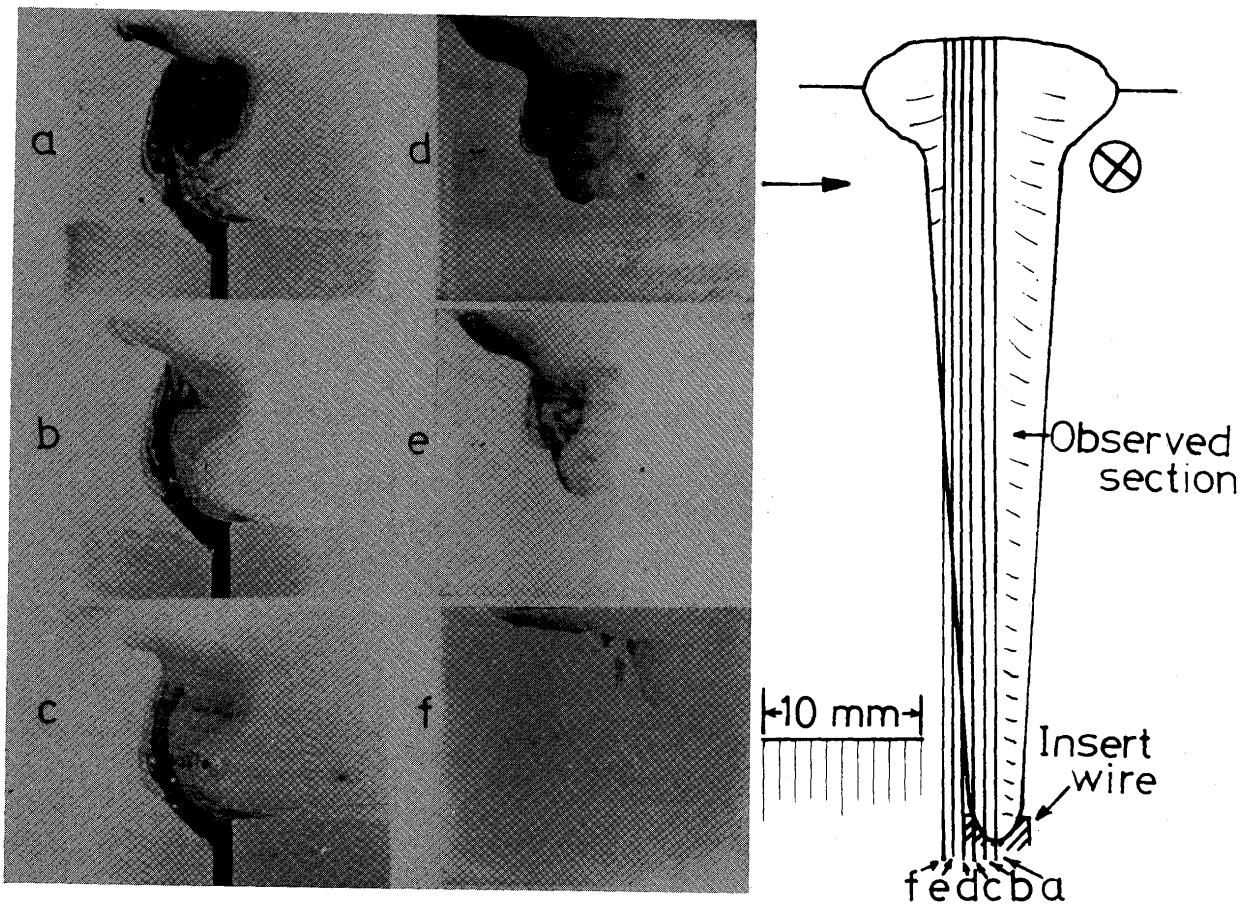

Fig. 7. An example of inflow of stainless steel molten metal to carbon steel weld metal.

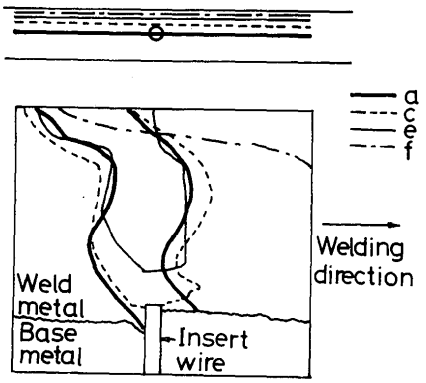

Fig. 8. Schematic representation of distribution of stainless steel molten metal in weld metal.

direction. Also from observing the deepness of color in photograph, it is clear that the latter is deeper. It is considered this means as follows; most of molten metal which rises from lower part along solidification interface turns at this position and flow ahead with the progress of welding. Fig. 9 shows the schematic diagram of this matter.

The inclination above mentioned is also seen clearly in Fig. 7 (b) besides in Fig. 7 (a). Moreover, from **Fig. 9** it is understood molten metal is not mixed completely. In order to investigate this phenomenon the authors studied when welding of thick plate, to

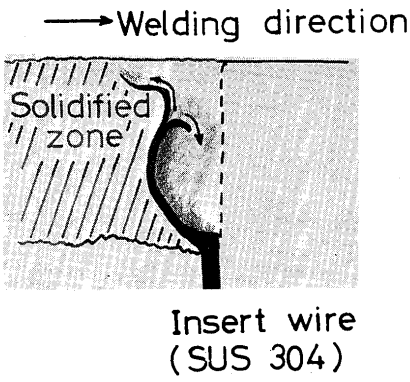

Fig. 9. Schematic diagram of two kinds of flow in molten metal.

what position was mixed the insert metal of any position after welding.

In this experiment we applied carbon steel plate (thickness: 40 mm) as base material and nickel sheet (thickness: 0.5 mm) as a insert metal because nickel forms a complete solid solution with iron, melting point changes little when forming alloy and other physical characteristics correspond comparatively to iron. Thus we fixed nickel sheet completely to bottom, center and surface of carbon steel base metal by TIG arc welding, and carried bead-on-plate welding without filler metal by electron beam welding. After welding we observed transverse section of test specimen using microscope and measured quantity of nickel in weld metal by X-ray probe microanalyzer (EPMA).

Fig. 10 shows an example of schematic diagram of distribution of nickel in weld metal observing by microscope. **Fig. 11 (a), (b),** and **(c)** also show the results of EPMA.

From Figs. 10 and 11 the following conclusions are summarized;

1) When set nickel sheet at the bottom of base metal, it rises along boundary zones of molten metal.
2) Nickel does not mix homogeneously regardless of the position of nickel sheet and the peak of deepness is seen in the neighborhood of nickel setting position.

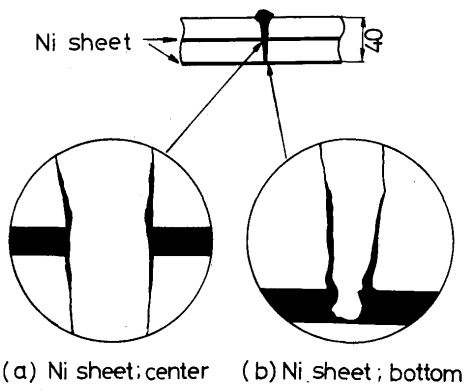

Fig. 10. Macro-sketch of weld bead section at different position of Ni sheet inserted.

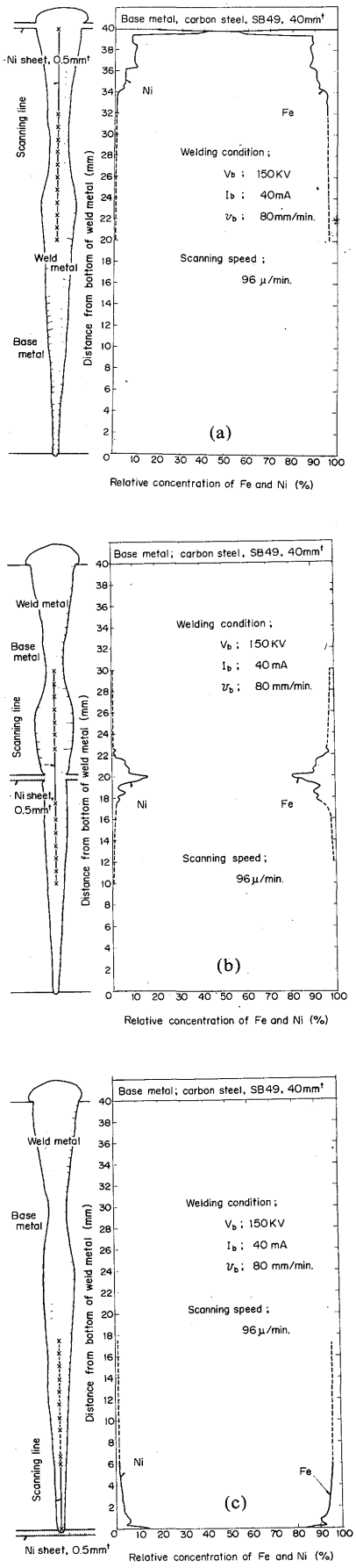

Fig. 11. Distribution of Ni and Fe contents by EPMA.

5. Relation between Dynamic Behavior of Molten Metal in Weld Molten Surface and Bead Ripple and Spiking

In this chapter the authors photographed the variation of molten metal in weld molten surface using a high speed camera, observed its dynamic behavior and discussed the relation between these results and bead ripple and spiking.

We carried out bead-on-plate welding on carbon steel, SB49 plate (thickness: 40 mm) with various welding conditions and photographed the behavior of bead surface in welding using a high speed camera (HYCAM).

Frame speed in photographing is about 2,500 frames/sec. from reserve experiment. An example of the results is shown in **Fig. 12** as a schematic diagram.

We observed the pictures photographed by a high speed camera using analysis machine (FILMOTION) and understood clearly that swellings occured periodically at the surface of weld molten pool. On the other hand it was seen many small bead ripples and comparatively big periodic bead ripples on the same weld bead surface as shown in **Photo. 3.** Also it was seen spikings as shown in **Photo. 4** when cutting the

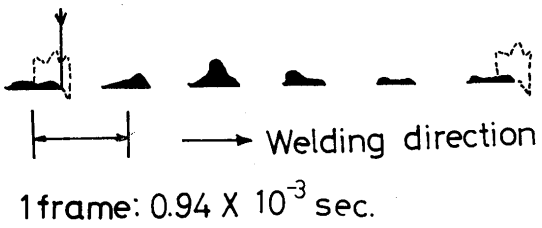

Fig. 12. Interrupted sketch of negative film photographed by high speed camera.

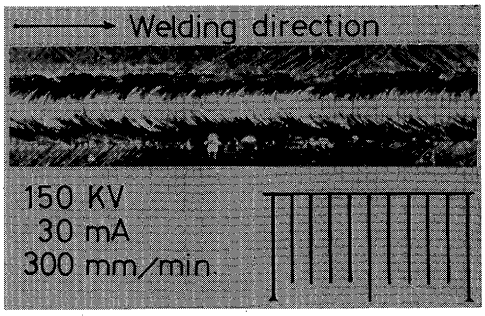

Photo. 3. Appearance of weld ripples at bead surface.

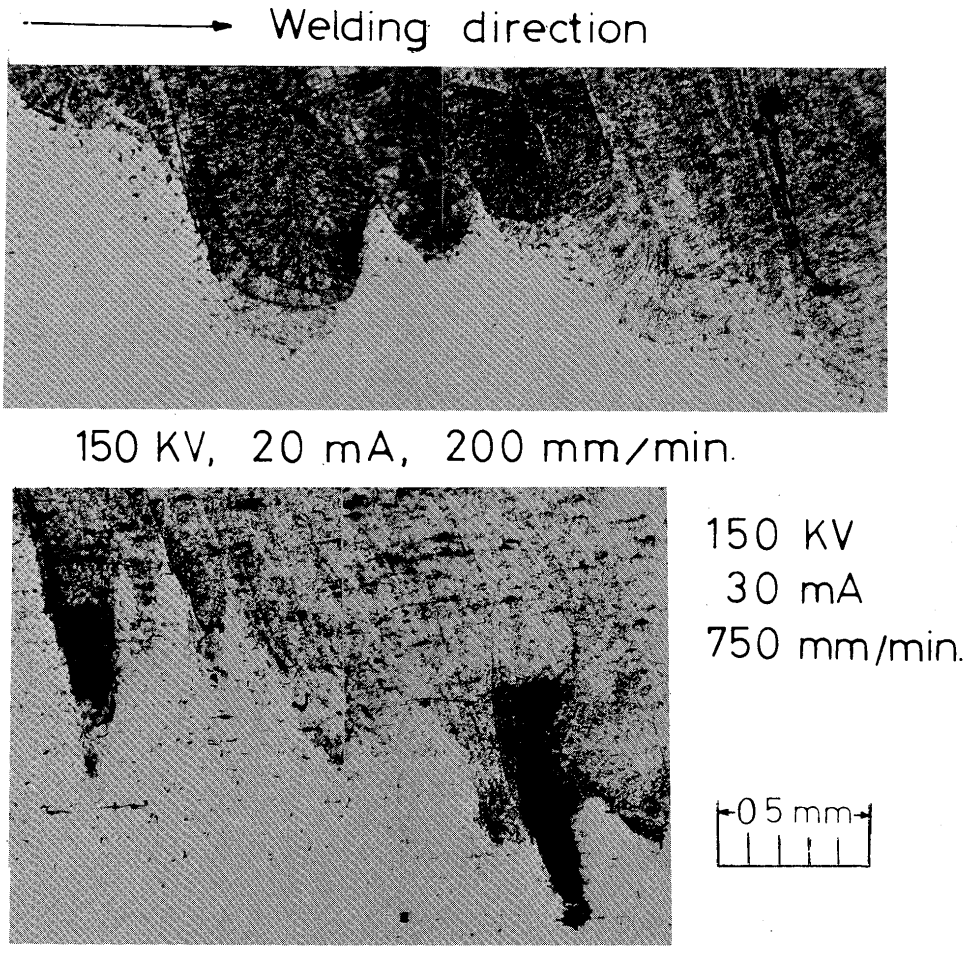

Photo. 4. Examples of spiking at longitudinal weld bead section.

same bead in longitudinal section and macro-etching. So the authors expected that the swellings in weld molten pool as seen by high speed camera and bead ripples and spikings were closely concerned and discussed these relations. First the authors measured maximum height of swellings of weld molten pool occuring periodically. These results are shown in **Figs. 13, 14** and **15,** arranging by welding speed (v_b) and welding heat input ($V_b \cdot I_b / v_b$).

These results are shown selecting measured points of 50 from data and also including variations.

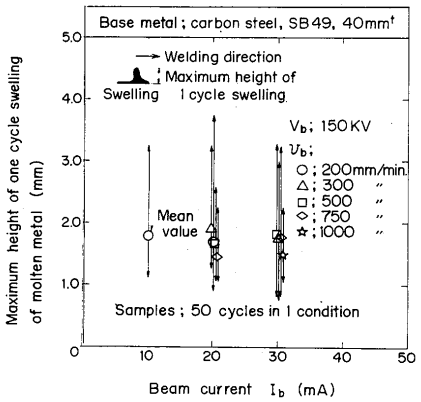

Fig. 13. Effect of beam current on surface swellings of molten metal during welding.

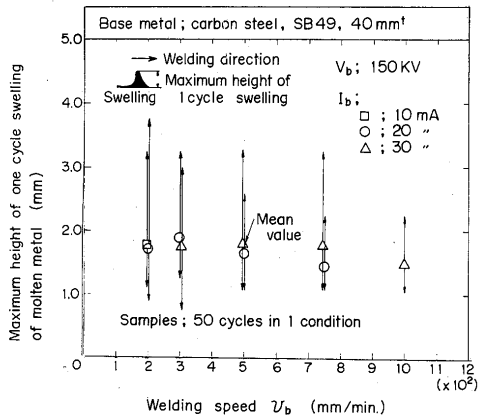

Fig. 14. Effect of welding speed on surface swellings of molten metal during welding.

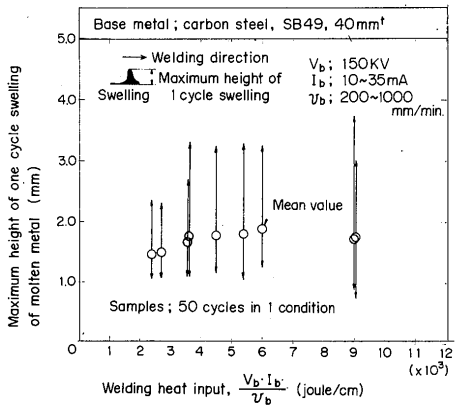

Fig. 15. Effect of welding heat input on surface swellings of molten metal during welding.

From these results it became clear that the mean value of maximum height of swellings was almost constant regardless of these parameters. However, regarding the maximum value shown in arrow mark it is not always constant, for example in the case of small welding heat input it took very small value as shown in Fig. 15. This means the maximum height of swellings decreases with small penetration depth. **Fig. 16** shows the relation between numbers of surface swellings (No./mm) and welding speed. In this figure the maximum height of swellings are divided three stages ($\geqq$2.0, $\geqq$2.5, $\geqq$3.0). We applied welding current of 10, 20 and 30 mA in this experiment. From this results it is seen that the numbers of swellings which indicates the same height decreases as welding speed increases except the low welding speed (200 mm/min.). This will be due to decreasing of penetration depth as mentioned above.

Next the authors measured the numbers of ripples in weld bead surface and spikings in the point of weld penetration and studied the relation between average numbers per 1 mm and welding speed, welding current and welding heat input. This result is shown in **Figs. 17** and **18.**

As to the numbers of ripples we studies about the both (R) and (R'), the former (R) are periodical, rough and deep ripples and the latter (R') are shallow ripples. From these results it is understood that the numbers (No./mm) of spikings and the rough ripples (R) are nearly equal and they change little regarding welding speed, welding current and welding heat input. These values are from 2 to 4 per mm. That is, it is considered that the periods of spikings and rough ripples (R) are also the same. On the contrary the numbers (R+R') incline to decrease gradually as increasing welding speed and satulate to constant values as shown in Fig. 16. However the inclination regarding welding current can be regarded approximately

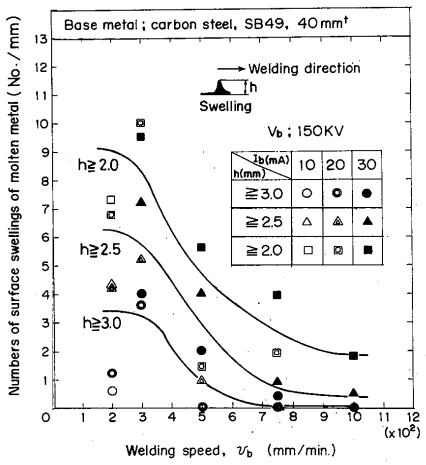

Fig. 16. Effect of welding speed on numbers of surface swellings of molten metal.

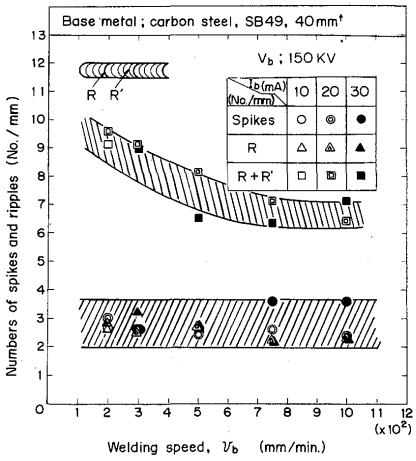

Fig. 17. Effect of welding speed on occurances of spikings and bead ripples.

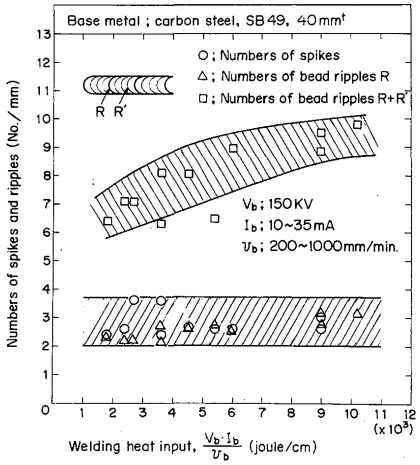

Fig. 18. Effect of welding heat input on occurances of spikings and bead ripples.

nearly constant. Accordingly the numbers (R+R') increase gradually as increasing welding heat input. Thus numbers of shallow ripples (R') vary a little in accordance with welding conditions. From the results of Fig. 17 and Fig. 18, it is understood the periods of spikings and rough bead ripples (R) are nearly equal. Accordingly next we arranged again Fig. 16 regarding welding heat input and added to Fig. 18. The result is shown in **Fig. 19.** In this figure we divided maximum height of swellings which measured by high speed film in three stages ($h \geqq 3.0$, $\geqq 2.5$ and $\geqq 2.0$ mm) and showed in a graphic form regarding welding heat input.

From this result it is understood that muximum height of swellings which indicate the same period with spikings and rough bead ripples (R) correspond to the curve of $h \geqq 3.0$ mm in the welding heat input of more than about 5,000 Joule/cm. Also they correspond to the curve of $h \geqq 2.5$ mm in the welding heat input of about 4,000—5,000 Joule/cm and to

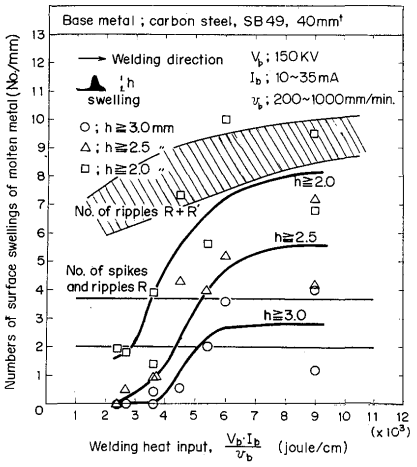

Fig. 19. Effect of welding heat input on numbers of surface swellings of molten metal during welding.

$h \geqq 2.0$ mm in the small welding heat input. Thus it is understood that the maximum height of swellings which correspond to the periods of spikings and rough bead ripples (R) decrease as decreasing of welding heat input. This is expected that as decreasing of welding heat input penetration depth decreases, so the maximum height of swellings lowered gradually and bead ripples and spikings are formed with this lower swellings. That is, it is considered that as welding heat input decreases the maximum height of swellings of weld molten metal which form rough bead ripples and spikings lower gradually.

The results obtained in this chapter are summarized as follows;

1) From the observation of high speed film, weld molten metal swelles dynamically by about constant periods. That is, the periodical variations occur in the surface of weld molten pool.
2) It was seen a certain relations between the numbers of swellings in weld molten metal and bead ripples and spikings. Namly, the periods whose maximum height of swellings take more than a certain value and the periods of rough bead ripples and spikings corresponded approximately. According to these results, it is considered that the variations of the surface in weld molten pool are connected closely to the shape of bead ripples and spikings.

6. General Discussions about the Dynamic Behaviors of Molten Metal in Weld Molten Pool

As mentioned above the authors studied some experiments about the dynamic behaviors of weld molten metal in 2-5 chapters. From these results the dynamic behaviors of weld molten metal during electron beam welding are expected as shown in **Fig. 20.**

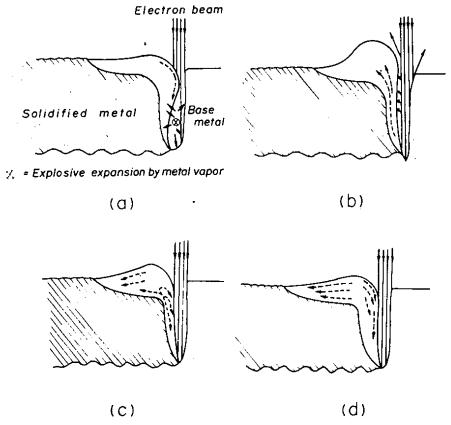

Fig. 20. Schematic representation of expected dynamic behavior of molten metal during electron beam welding.

The discussions in Fig. 20 are summarized as follows;

(a) Molten metal near the surface acts to close a hole due to self weights of molten metal itself. Then upper parts of a hole are narrowed, so the inrush of electron beam to the piercing hole as well as the discharges of vapor metal and gas are becoming trouble. On the other hand inner vapor metal and gas are continuously heated because of electron beam entered through small opening, therefore a great deal of the vapor metal and the gas which are expanded by heating is eager to escape through the opening. Moreover concentrated electron beam in the core zone abruptly superheat and vaporize the inner surface of the narrowing hole when overhanging of molten metal is excessively advanced. By the two kinds of force in above the expansion occurs suddenly in the hole at a critical diameter.

(b) Due to expansion in (a), wall of molten metal is pushed and Fig. (b) is formed and when at this time molten metal in under parts is rised along solidification interface. Also at the same time a big swelling of molten metal is formed gradually in the surface of weld bead. Again as the result of extending of the hole, most of electron beam concentrate to the bottom of the hole and spiking occurs.

(c) Next swelling of molten metal rised up begins to lower again by the pressure of molten metal itself. At this time the flow of weld molten metal rised up from the bottom branches to two flows at the bending position and the one part passes to upper side and the other most of part turns at the bending position and falls to the bottom of the hole with the general motion of molten metal.

(d) Progressing from the stage (c), swelling of molten metal lowers and begins to close the opening of the hole gradually. And molten metal generally begins to fall to the bottom of the hole.

After stage (d), stage (a) begins again, the opening of the hole is narrowed, next the expansion occurs suddenly in the hole and swelling of molten metal occurs. Again following to this, spiking and rising action of molten metal occurs. Also it is considered that in the interval of big variations in molten pool, a little vibrations occur at the surface of molten metal and shallow bead ripples are formed.

The above mentioned are the explanations of dynamic behaviors of molten pool during electron beam welding obtained as the results in this studies.

7. Conclusions

The results obtained in this studies summarized as follows;

(1) The penetration shape in electron beam welding could be photographed directly on X-ray film. As the result it became clear that X-ray occured corresponding to the penetration shape and more strong X-ray occured at the position of spiking. From this results it was understood that electron beam did not always go to base metal continuously, but discontinuously and spiking could be formed by the strong electron beam.

(2) The authors could extrude molten metal in welding and expose the solidification interface using instantaneous extrusion method. Then as the result it became clear that ripple lines which were seen in the longitudinal section of weld bead almost corresponded to the shape of solidification interface. So it became to be able to expect the solidification interface by the ripple lines. Also concerning weld beads of the same welding condition, it became clear that solidification interface did not show always the same form but varied differently.

(3) The authors set an insert metal in weld molten pool and studied the dynamic behaviors of molten metal observing the flow of insert metal. As the results it was understood that molten metal in the bottom of penetration raised along the solidification interface, branched to two flows at the bending position, the one part passed to upper side, but the other most of part turned at the bending position and fell to the bottom of the hole. This results are very important to make clear the dynamic behavior of weld molten pool. Also it became clear that weld metal did not mix homogeneously.

(4) The authors observed the dynamic behaviors of molten pool at the surface of weld bead by high

speed picture and studied the relation between the results observed above and spikings and bead ripples.

From this results we understood that weld metal in welding varied periodically and swellings of molten metal occured by a certain interval. Also it became clear that the periods of swellings of molten metal and spikings and bead ripples are connected closely.

In this experimental results the periods of spikings and deep bead ripples were almost equal and the value almost corresponded to the periods of the swellings which had the height of more than 3.0 mm in the condition of welding heat input of 5,000 Joule/cm. Also it was understood when welding heat input lowered maximum height of swellings whose period corresponded to spikings and bead ripples decreased generally because of small penetration.

(5) Synthesizing the results obtained from various experiments mentioned above, the authors showed the periodical dynamic behaviors of molten pool in electron beam welding to a schematic diagram.

Acknowledgement

The authors would like to express Dr. Kiyoshi Terai and Mr. Hiroyoshi Nagai of Kawasaki Heavy Industries, Ltd. and Mr. Eiske Yamamoto and Mr. Kazuo Isoura of Osaka Transformer Co. Ltd. for their co-operations.

References

1) T. Hashimoto and F. Matsuda: Trans of NRIM, 7 (1965).
2) H. Tong: Heat transefer and cavity penetration during electron beam welding, Department of mechanical engineering davis, California Report No. 69-14 (1969).
3) C. M. Webar, E. R. Funk and R. C. McMaster: Penetration mechanism of partial penetration electron beam welding W.J. 2 (1972).
4) N. Taniguch and T. Miyazaki: Experimental analisis on the deep penetration of electron beam paper presented at the CIRP general assembly, Stockholm (1972).
5) K. Nakane et al: EBW-67-72, (1972).